HHS Public Access

Author manuscript

Oncogene. Author manuscript; available in PMC 2021 August 16.

Published in final edited form as:

Oncogene. 2020 January ; 39(4): 877–890. doi:10.1038/s41388-019-1029-6.

Bile acid-induced "Minority MOMP" promotes esophageal carcinogenesis while maintaining apoptotic resistance via Mcl-1

Yuan Xu[1], **Deborah R. Surman**[1,2], **Laurence Diggs**[1], **Sichuan Xi**[1], **Shaojian Gao**[1], **Devikala Gurusamy**[3], **Kaitlin McLoughlin**[1], **Justin Drake**[1], **Paul Feingold**[1], **Kate Brown**[1], **Danny Wangsa**[4], **Darawalee Wangsa**[4], **Xi Zhang**[5], **Thomas Ried**[4], **Jeremy L. Davis**[1], **Jonathan Hernandez**[1], **Chuong D. Hoang**[1], **Rhonda F. Souza**[5], **David S. Schrump**[1], **R. Taylor Ripley**[1,2]

[1]Center for Cancer Research, National Cancer Institute, NIH, Bethesda, MD, USA

[2]Division of General Thoracic Surgery, Michael E. DeBakey Department of General Surgery, Baylor College of Medicine, Houston, TX, USA

[3]Surgery Branch, Center for Cancer Research, National Cancer Institute, NIH, Bethesda, MD, USA

[4]Genetics Branch, Center for Cancer Research, National Cancer Institute, NIH, Bethesda, MD, USA

[5]Department of Medicine, Center for Esophageal Diseases, Baylor University Medical Center and Center for Esophageal Research, Baylor Scott and White Research Institute, Dallas, TX, USA

Abstract

Barrett's esophagus (BE) is associated with reflux and is implicated the development of esophageal adenocarcinoma (EAC). Apoptosis induces cell death through mitochondrial outer membrane permeabilization (MOMP), which is considered an irreversible step in apoptosis. Activation of MOMP to levels that fail to reach the apoptotic threshold may paradoxically promote cancer—a phenomenon called "Minority MOMP." We asked whether reflux-induced esophageal carcinogenesis occurred via minority MOMP and whether compensatory resistance mechanisms prevented cell death during this process. We exposed preneoplastic, hTERT-immortalized Barrett's cell, CP-C and CP-A, to the oncogenic bile acid, deoxycholic acid (DCA), for 1 year. Induction of minority MOMP was tested via comet assay, CyQuant, annexin V, JC-1, cytochrome C subcellular localization, caspase 3 activation, and immunoblots. We used bcl-2 homology domain-3 (BH3) profiling to test the mitochondrial apoptotic threshold. One-year exposure of Barrett's cells to DCA induced a malignant phenotype noted by clone and tumor formation. DCA promoted minority MOMP noted by minimal release of cytochrome C and limited caspase 3 activation, which resulted in DNA damage without apoptosis. Upregulation of the antiapoptotic protein, Mcl-1, ROS generation, and NF-κB activation occurred in conjunction with minority MOMP. Inhibition of ROS blocked minority MOMP and Mcl-1 upregulation. Knockdown of Mcl-1 shifted

R. Taylor Ripley, R.Taylor.Ripley@bcm.edu.

Conflict of interest The authors declare that they have no conflict of interest.

Supplementary information The online version of this article (https://doi.org/10.1038/s41388-019-1029-6) contains supplementary material, which is available to authorized users.

minority MOMP to complete MOMP as noted by dynamic BH3 profiling and increased apoptosis. Minority MOMP contributes to DCA induced carcinogenesis in preneoplastic BE. Mcl-1 provided a balance within the mitochondria that induced resistance complete MOMP and cell death. Targeting Mcl-1 may be a therapeutic strategy in EAC.

Introduction

Esophageal cancer affected 17,000 patients and caused 16,000 deaths in 2018 [1]. Prognosis for patients with metastatic disease is particularly grim with 5-year survivals under 15% [2]. The incidence of esophageal adenocarcinoma (EAC) has risen dramatically [3]. Chronic gastro-esophageal reflux disease (GERD) affects more than 20% of adults in the United States [4], which leads to Barrett's Esophagus (BE). BE is a premalignant condition with the highest associated risk for EAC. Gastric refluxate includes gastric secretions and bile salts [5]. Certain bile acids such as deoxycholic acid (DCA) transform the normal squamous epithelium to columnar epithelium resulting in the transition from low to high grade dysplasia which may ultimately result in EAC [6]. Although the relationship between bile reflux and EAC has been well established, little is known about the mechanisms that link bile acids to esophageal carcinogenesis. We developed an in vitro, long-term exposure model to study the mechanisms by which bile acids drive EAC initiation, progression, and resistance.

"Minority MOMP" is the sublethal activation of the intrinsic pathway of apoptotic machinery that promotes genomic instability, cellular transformation, and tumorigenesis [7, 8]. The key event is mitochondrial outer membrane permeabilization (MOMP), in which Bax and Bak1 [9], membrane channel proteins, colocalize to the outer mitochondrial membrane (OMM). These proteins generate proteolipid pores that enable MOMP [10] which is the irreversible step in apoptosis. MOMP releases toxic proteins such as cytochrome C (cytoC) and endonuclease G (EndoG) from the mitochondrial inner membrane (MIM) space into the cytoplasm, which activates the caspase system [11]. Following sublethal stresses, cells may survive when small percentages or a minority of mitochondria undergoes MOMP. This self-limiting MOMP leads to cytoC release and caspase activation below the threshold necessary to trigger apoptosis resulting in caspase-mediated DNA damage without cell death—"Minority MOMP."

Resistance to apoptosis is a well-established hallmark of cancer [12]. MOMP is a switch-like event regulated by the balance of antiapoptotic and proapoptotic B-cell lymphoma 2 (Bcl-2) family members. While the activity of antiapoptotic members, such as Bcl-2, Bcl-xL, and Mcl-1, raises the threshold for MOMP, the proapoptotic proteins, such as BIM, BIM, BAD, and PUMA, reduce it [13, 14]. Toxic stimuli may make cells more susceptible to MOMP; however, cells may withstand stressful stimuli and avoid apoptosis by upregulating antiapoptotic proteins. Paradoxically, those cells may sustain sufficient damage to promote carcinogenesis. In minority MOMP, the partial but persistent induction of the caspase system may require compensatory upregulation of the antiapoptotic proteins in order to survive sustained insults, such as toxic exposure, to bile acids.

We developed a 1-year exposure model of preneoplastic Barrett's cells to the oncogenic bile acid, DCA, and examined the counterintuitive hypothesis that minority MOMP facilitates cellular transformation and carcinogenesis while promoting resistance to apoptosis. We asked whether chronic exposure to DCA reprograms the delicate balance of Bcl-2 family members to maintain minority MOMP. This mechanism may provide potential strategies to disrupt this balance with novel therapeutic options that convert minority MOMP to complete MOMP.

Results

The bile acid, DCA, induces carcinogenesis in dysplastic Barrett's epithelial cells

Our previous data showed that acute exposure to DCA promoted an aggressive phenotype of EAC cells (EACC) [15]. To further investigate, CP-C (Barrett' s esophageal) cells were exposed to 100 μM DCA or DMSO control for 12 months (Fig. 1a). Clone formation in DCA transformed (DCA-T) cells formed as many clones as the positive control, OE33, while no clones grew in DMSO control (Fig. 1b). Three of five mice inoculated subcutaneously with DCA-T cells developed tumors compared with no tumors in controls (Fig. 1c). We observed significant increases in invasion and migration in DCA-T cells (Fig. 1d, e). Time-dependent increases in the oncogenic protein, c-MYC, paralleled the increases in the malignant phenotype (Fig. 1F). These phenotypic changes were also found in CP-A lines (Supplementary Fig. 1). Collectively, these findings suggest that long-term exposure to DCA promotes malignant transformation of BE cells to cancer cells. After these cells transformed to cancer cells, they were not expose to DCA.

DCA induces "Minority MOMP" in transformed BE cells

DNA damage is an important early step during carcinogenesis; therefore, we asked whether DCA exposure was associated with DNA damage in DCA-T cells We observed comet tails and phosphorylation of H2AX indicating DNA fragments and damage, respectively (Fig. 2a). To determine whether DNA damage resulted in chromosomal aberrations, we performed array CGH (aCGH) and spectral karyotyping (SKY). Difference in copy number alteration between DCA and DMSO was observed and the SKY results concurred with the aCGH, though no translocations were unique to DCA (Supplementary Fig. 2). Normally, DNA damage and genomic instability occur from activation of the apoptotic mechanisms. Therefore, we checked the apoptotic effector proteins of MOMP, Bax, and Bak1 and noted increased protein expression at 12 months (Fig. 2b). Interestingly, we tested apoptosis and proliferation and noted no change in DCA-T cells compared with controls (Fig. 2c, d). Bax and Bak1 normally act to induce MOMP and thus apoptosis. However, in our transformed model, we did not observe either apoptosis or cell number decreased. Therefore, we asked how these cells survive when the intrinsic apoptotic pathway is activated.

MOMP is associated with mitochondrial membrane depolarization ($\Delta\Psi m$), which we tested and observed that DCA resulted in decreased red to green ratio by JC-1 dye indicating that mitochondrial depolarization is present and consistent with at least partial MOMP (Fig. 2e). MOMP releases cytoC and EndoG from the MIM space into the cytoplasm; we noted a small increase in the cytosolic fraction of DCA-T cells compared with controls (Fig. 2f).

Next, we asked whether this low level of cytoC and EndoG could activate the caspase system. We tested cytoC activity in cytosol by ELISA and observed a 25% increase in the DCA-T cells. The positive control for MOMP, Actinomycin D, induced 80% cytoC increase (Fig. 2f). To further quantify the activation levels of caspase 3, we transduced a caspase 3 reporter that links a ubiquitin domain to GFP and luciferin signals by a caspase 3 cleave motif [8]. With activation of MOMP, the caspase 3 reporter site is cleaved and the GFP and Luciferase activity is detectable. Without MOMP, this construct is marked for proteasome degradation and no GFP or luciferase activity is detected. Both positive controls, ABT-263 (Inhibits the anti-apoptotic protein, Bcl-2) and MG132 (inhibits the proteasome), displayed high GFP signal and luciferase activities. In DCA-T cells, the GFP fluorescence and bio luminescence values were significantly increased by 25% compared with DMSO control, but not as robustly as the positive controls (Fig. 2g). Collectively, the upregulation of Bax and Bak1, the decrease in mitochondrial membrane potential, the slight release of cytoC and EndoG, and the low-level activation of the caspase system combined with DNA damage and absent cell death are indicative of “Minority MOMP” (CP-A— Supplementary Fig. 3).

Altered mitochondrial function and global metabolomic signatures in DCA transformed BE cells

Given that the mitochondria play a central role in respiration and energy production (oxidative phosphorylation (OXPHOS)), and alterations in mitochondrial metabolism can determine the predisposition or “priming” toward either cell death or survival, we asked whether the changes consistent with minority MOMP were also associated with changes in OXPHOS. The oxygen consumption rate (OCR) was measured using the Seahorse XF^e96 analyzer and we observed increases in maximal mitochondrial respiration and spare respiratory capacity in DCA-T cells (Fig. 3a and Supplementary Fig. 4). We tested the glycolytic pathway by measuring the extracellular acidification rate (ECAR) and did not observe significant differences (Supplementary Fig. 5). Mitochondria are the main source for endogenous reactive oxygen species (ROS), therefore, we asked whether the increases in OXPHOS were associated with increase in ROS and noted significant increases (Fig. 3b, c). These data suggest that bile acid drives OXPHOS and ROS production preferentially in DCA-T cells.

To further characterize metabolic alterations, global metabolomic analysis was performed and 68 significantly differential metabolites were identified between the DCA and DMSO groups (47 increased; 21 decreased) (Fig. 3d and Supplementary Table S1). We used the MetaboAnalyst tools to link metabolites to metabolic pathways. The pathway analysis found that glycogenesis, nucleotide sugars metabolism, Warburg effects, tricarboxylic acid (TCA) cycle, and malate-aspartate shuttle were significantly changed in DCA-T cells (Fig. 3e). Based on the pathways of interest and focusing on biological significance and informatics analysis, we explored the glycolytic and TCA cycle metabolic networks (Fig. 3f). The levels of citrate, *cis*-aconitate, fumarate, and malate were increased in DCA-T cells compared with controls, which indicate that TCA cycle is enhanced. The increase in TCA cycle metabolites was accompanied by increased energy NADH production, which is consistent with increased OCR (Supplementary Fig. 6). In summary, global metabolite analysis confirmed that

OXPHOS and the TCA cycle of the mitochondria are significantly activated in DCA-T cells.

ROS production is linked with “Minority MOMP”

Given that overproduction of ROS is associated with survival and malignancy, the effects of minority MOMP and ROS may overlap. Therefore, we explored whether DCA-induced minority MOMP is associated with ROS production. After pretreatment with the antioxidant N-acetylcysteine (NAC), the intracellular ROS content decreased significantly as expected (Supplementary Fig. 7A). Next, we explored whether blocking ROS production can reverse DCA-induced minority MOMP. As noted previously, cell proliferation was similar in DCA-T and DMSO groups; however, when the cells were pretreated with NAC, cell proliferation significantly decreased in the DCA-T group (Fig. 4a and Supplementary Fig. 7B). Similarly, in the DCA-T group, the clone numbers were significantly decreased with ROS inhibition (Fig. 4b). Blockage ROS generation decreased cell apoptosis in both groups. However, in DCA-T cells, NAC treatment significantly increased apoptosis compared with DMSO groups. These findings suggest that minority MOMP may protect the cells from the toxic effects of DCA, which implicate minority MOMP in the resistance mechanisms of the cells (Fig. 4c).

To further explore the link between ROS and minority MOMP, ΔΨm, cytoC, and caspase 3 activities were tested. ΔΨm drops with minority MOMP, however, this drop-in membrane potential was lost with NAC (Fig. 4d). In addition, the release of cytoC into the cytosol and the low-level caspase 3 activation were also blocked by NAC (Fig. 4e, f). Finally, DNA damage was abrogated noted by no γH2AX increase with NAC (Fig. 4g). These results indicated that DCA-induced minority MOMP is tightly linked to ROS generation. Therefore, we explored whether ROS generation maintain the balance in Bcl-2 family that controls minority MOMP.

Mcl-1 provides a balance to bile acid-induced minority MOMP

We found that the proapoptotic effector proteins that form OMM pores, Bax and Bak1, were upregulated in DCA-T cells but that cell death did not occur. This finding, combined with the results above, suggests that minority MOMP has occurred. Therefore, we blocked Bax and Bak1 expression and noted that their absence did not completely reverse minority MOMP (Supplementary Fig. 8). These findings suggested that DCA may alter both the pro- and anti-apoptotic machinery of the Bcl-2 family that prevents minority MOMP from shifting to complete MOMP.

We performed bcl-2 homology domain-3 (BH3) profiling by titrating proapoptotic peptides that correspond to the binding domains of the respective proteins (BH3 peptides) while measuring relative cytoC release. We expected that DCA-T cells would be more primed based on induction of minority MOMP; however, they were far less primed compare with DMSO cells. They required higher doses of BIM, PUMA, BAD, and HRK BH3 peptides to trigger cytoC release (Fig. 5a). We postulated that increases in the antiapoptotic proteins countered the effects of the proapoptotic effector proteins, Bax and Bak1. We screened the BCL-2 family and noted that Mcl-1, an antiapoptotic protein, was significantly increased

whereas no changes in Bcl-2, Bcl-xL, BIM, or BID occurred (Fig. 5b and Supplementary Fig. 9A). Given that blocking ROS with NAC abrogated minority MOMP, we asked whether ROS inhibition prevented Mcl-1 upregulation and, indeed, we observed complete abrogation of Mcl-1 upregulation with NAC (Fig. 5b and Supplementary Fig. 9). These findings suggest that DCA-induced minority MOMP does not shift the cells toward apoptosis, rather, DCA induces compensatory changes that protect from death. DCA induces oncogenic mechanisms simultaneously with resistance mechanisms.

We further explored the role of Mcl-1 by knocking down Mcl-1 in DMSO and DCA-T cells. We observed that the increase in Mcl-1 expression was almost totally blocked by the knockdown in DCA-T cells but had no effects on BAX and BAK1 expression (Supplementary Fig. 10). Similar to abrogating ROS, knockdown of Mcl-1 decreased cell proliferation and increased apoptosis in DCA-T cells but not in the control group (Fig. 5c, d). These findings suggested Mcl-1 is critical to preventing apoptosis in DCA-T cells and that blockage of Mcl-1 disrupts the balance that enables minority MOMP.

To further explore whether blocking Mcl-1 could shift DCA-induced minority MOMP to complete MOMP, caspase 3 activity, cytoC release, $\Delta\Psi m$, and BH3 profiles were tested. First, cleaved-caspase 3 was slightly increased with DCA for shCTL as expected; however, with Mcl-1 knockdown, caspase 3 activation was substantially larger (Fig. 5e). Next, we noted that the cytosolic fraction of cytoC was significantly increased with Mcl-1 inhibition (Fig. 5f). In DCA-T cells with Mcl-1 knockdown, DCA induced-mitochondrial depolarization was blocked (Fig. 5g). Finally, we explored the effects of Mcl-1 on mitochondrial priming by BH3 profiling. We observed that blockage of Mcl-1 expression did not change the mitochondrial priming in the control group; however, in DCA-T cells, knockdown Mcl-1 substantially increased the sensitivity to BH3 peptides (Fig. 5h). For example, with knockdown of Mcl-1, the percentage of cytoC release by BAD was much higher. These findings suggest that Mcl-1 upregulation is critical to maintain the “unprimed” mitochondria during minority MOMP. These findings suggest that Mcl-1 plays a critical role in resistance mechanisms during bile acid-induced minority MOMP.

Mcl-1 is expressed in most esophageal cancer tissue samples and is associated with poor patient prognosis

To investigate an association of Mcl-1 with human EAC, we utilized a tissue microarray to examine Mcl-1 expression in normal esophagus and tumor specimens (Fig. 6a). Although not statistically significant, Mcl-1 was expressed in many of the tumors. In addition, we tested other antiapoptotic proteins, Bcl-2 and Bcl-xL, and the expression was much lower compared with Mcl-1 (data not shown). We queried The Cancer Genome Atlas and noted that higher Mcl-1 expression was associated with reduced overall survival in EAC patients (Fig. 6b). Bcl-2 and Bcl-xL expression did not correlate to differences in patient survivals. These findings suggest that this target may be appropriate for a precision-based appropriate to certain patients with Mcl-1 positive tumors.

Inflammation and NF-κB activation contribute to Mcl-1 upregulation

We performed global gene expression analysis and observed 475 significantly differentially-regulated genes (263 genes increased; 212 genes decreased) in DCA-T cells with an average expression level >1.5-fold (P <0.05, Supplementary Table S2). Ingenuity Pathway Analysis (IPA) demonstrated that the most frequently involved canonical pathways included proinflammatory cytokine production, including LPS/IL-1, HMGB1, IL-8, and IL-17 signaling (Fig. 7a and Supplementary Table S3). Gene Set Enrichment Analysis (GSEA) identified several significantly enriched gene set that correlated with genes induced by DCA exposure (Supplementary Fig. 11A). The genes associated with a role in an inflammation pathway were graphed, the heatmap plots showed a set of 18 genes involved in inflammation (Fig. 7b). We used qRT-PCR to confirm the expression of several inflammatory genes including IL-6, IL-1A, and IL-8 (Fig. 7c). IPA and confirmatory mRNA expression indicate that DCA induces the inflammation processes in EACC.

Given that ROS are involved in inflammatory disorders and are increased in DCA-T cells, we asked whether ROS production was critical to DCA-induced inflammation. We observed that blocking ROS generation with NAC completely blocked the DCA-induced increase in cytokine expression (Fig. 7d). Given that the transcription of NF-κB-dependent genes influences the levels of ROS, and in turn, the levels of NF-κB activity are also regulated by the levels of ROS, we explored NF-κB activity. Based on the GSEA analysis, we noted that the NF-κB signaling pathway was highly enriched in DCA-T cells (Supplementary Fig. 11B). Next, we tested the NF-κB signaling pathway and found that phosphorylated-p65 increased in DCA-T cells and was significantly abrogated by ROS inhibition (Fig. 7e, f). These findings imply that ROS generation, through mitochondrial alteration, acts as a mediator and is tightly linked to the DCA induced inflammatory processes.

As noted earlier, Mcl-1 increased with DCA exposure and decreased with ROS inhibition and NF-κB activation paralleled ROS generation. We explored whether NF-κB activation could contribute to DCA-induced Mcl-1 expression. We treated DCA-T with BAY117085 (inhibitor of an NF-κB pathway) and noted complete blockage of p-p65 induction. Moreover, the increase in Mcl-1 expression was significantly abrogated unlike Bax and Bak1 with NF-κB inactivation (Fig. 7g and Supplementary Fig. 12). These findings suggest that targeting the NF-κB signaling pathway can mimic decreases in ROS to prevent upregulation of Mcl-1 which can block resistance mechanisms induced during minority MOMP.

Discussion

In this study, we established a long-term exposure model to query whether bile acid can transform Barrett's cells and observed in vitro and in vivo changes consistent with transformation. We noted these effects started about 6 months and increased at one year. Bajpai et al. [16] noted a similar time course for malignant transformation when benign Barrett's epithelial cells (BAR-T) were exposed to bile and acid for 5 min per day for 1 year. The differences in the model are noteworthy because their group focused on the combination of 200 μM of DCA with a pH of 4 for a short exposure time. When we established our model, we found that dosages of DCA >100 μM of DCA resulted in

decreased viability with continuous exposure. The lack of effects on viability or proliferation are critical to the observations of minority MOMP, therefore, we established a model with no obvious toxic effects from DCA. Their model certainly has merit, however, given that EAC still occurs in patient treated with gastric acid inhibitors but for whom bile reflux is not reduced, we thought that a bile model without acid was an appropriate for GERD-treated patients. Importantly, the malignant transformation that Bajpai et al. was strikingly like our observations.

Resistance to apoptosis is a well-established hallmark of cancer [12] and, paradoxically, rescuing cells from apoptosis may promote cancer. Exposure of primary liver cells to ethanol caused the initiation then recovery from apoptosis which increased oncogenic transformation [17]. Another study found that sublethal doses of TRAIL led to caspase-dependent mutations and genomic instability in surviving cells [18]. We found that DCA-T cells activated the mitochondrial intrinsic apoptotic pathway but survived [8]. Tait et al. originally described this phenomenon as “Incomplete MOMP” and challenged that MOMP is a point-of-no-return that invariably results in cell death [10]. Extending these findings, Ichim et al. described this phenomenon as “Minority MOMP” [7]. They treated cells with the BH3-mimetic, ABT-737, and noted that limited, sublethal caspase activation could induce DNA damage that promoted genomic instability and cellular transformation [7]. We believe that DCA-induced minority MOMP, at least partially, accounts for the malignant transformation of the Barrett’s cells. While Bajpai et al. showed that prolonged acid and bile exposure could induce chromosomal aberrations and clonal selection in benign Bar-T cells that failed to repair DNA damage [16], the mechanism of resistance to apoptosis was unclear. Therefore, we explored a mechanism for resistance during DCA exposure that would enable cells to tolerate persistent DNA damage.

Given that our findings are consistent with minority MOMP, we postulated that the cells would be more primed to undergo apoptosis [19]. Yet, BH3 profiling suggested that DCA-T cells were less primed. We detected an increase in the Mcl-1 expression, which may explain this paradoxical finding. Mcl-1 overexpression has been linked to the pathogenesis of a variety of refractory cancers [20] and the critical role of Mcl-1 in apoptotic resistance has been highlighted by downregulating Mcl-1 protein levels with pharmacologic inhibition [21-24]. When we blocked Mcl-1, apoptosis occurred in DCA-T cells. In addition, the BH3 profile in the DCA-T cells suggested that the cells were closer to the apoptotic threshold without Mcl-1 expression. These findings indicate that Mcl-1 upregulation may provide a balance or a gate keeper function that enables minority MOMP while preventing apoptosis.

Mitochondria have a pivotal role in producing metabolites, byproducts of the TCA cycle, which can determine whether a cell proceeds toward survival or apoptosis [25, 26]. Since MOMP and Mcl-1 are tightly linked to the mitochondria, we explored changes in mitochondrial dynamics in the DCA-T cells to identify potential mechanisms to reprogram the mitochondria. We observed increases in OXPHOS and accumulation of TCA cycle intermediates. These findings are consistent with our previous data demonstrating that DCA could functionally reprogram the mitochondria to support the needs of progressive cancer cells [15]. Mitochondrial-derived ROS have been reported to be a major determinant of cell apoptosis [27, 28]. Anticancer agents that induced ROS production have been reported

to modulate mitochondrial function by causing loss of mitochondria membrane potential and leakage of cytoC and AIF [29]. In contrast, in DCA-T cells, we observed that ROS production was tightly linked to minority MOMP and attenuation of ROS with NAC disrupted this phenomenon. Inhibition of ROS with NAC has been reported to attenuate pristimerin-induced Bax activation and mitochondrial redistribution of Bax [30]. In addition, ROS has been reported to regulate multiple members of the Bcl-2 family [31, 32]. We found that NAC completely inhibited the increases in Bak1 and Mcl-1 expression by DCA. These findings suggest that ROS is involved in the underlying mechanisms by maintaining a balance in the Bcl-2 family. Moreover, double knockdown of Bax and Bak1 did not totally reverse DCA-induced minority MOMP, providing evidence that ROS alters both the pro- and anti-apoptotic machinery in the Bcl-2 family. These results provide a mechanism by which DCA-induced minority MOMP is protected from apoptosis through the upregulation of Mcl-1. Since ROS is tightly linked to inflammation, we explored the NF-κB pathway. Activation of NF-κB in chronic inflammation, like GERD, may promote the development of cancer. Huo previously reported that activation of NF-κB allows Barrett's metaplasia to resist apoptosis in the setting of DNA damage induced by UV-B irradiation [33, 34]. Our findings support these results in that activation of NF-κB in DCA-induced inflammation contributes to Mcl-1 overexpression. Targeting NF-κB may be an alternative strategy to directly targeting Mcl-1.

Collectively, our study provides a molecular mechanism for transformation of Barrett's esophageal cells to cancer via "Minority MOMP" (Fig. 8). This mechanism may be critically dependent upon upregulation of antiapoptotic proteins, such as Mcl-1. Pharmacological inhibition of Mcl-1 may be the most direct strategy to reestablish the cellular sensitivity to apoptosis in Mcl-1 expressing tumors. Recently, specific Mcl-1 inhibitors have been developed that may merit further clinical trials [35]. Mcl-1 inhibition may promote the shift of minority MOMP to cell death in bile reflux-related esophageal cancer.

Materials and methods

Cell culture and conditions

CP-C and CP-A are commercially available high- and low-grade Barrett's cell line [36], purchased from the ECACC (UK) authenticated with human leukocyte antigen (HLA) analysis by NIH-HLA laboratory every 3 months (Supplementary Table S4). Cells were cultured in RPMI media supplemented with 10% fetal calf serum and 1% penicillin/streptomycin. DCA was suspended in DMSO as stock concentration. The long-term exposure model was established in CP-C and CP-A cells exposed to either 100 μM DCA or DMSO control for 12 months with twice weekly media changes. Each condition was set up in triplicate and cultured independently.

Apoptosis

Cells were stained with annexin V and PI according to the manufacturer's instruction. After the cells were incubated at room temperature for 15 min in the dark, apoptotic cells were analyzed with FACS Caliber (Becton Dickinson, Heidelberg, Germany). Apoptotic cell

percentage corresponded to annexin V(+)/PI(−) cells. Data were analyzed using the FlowJo 10.4.1 software (Tree Star, USA).

JC-1 assays

Mitochondrial membrane potential (ΔΨm) changes were detected using the mitochondrial membrane potential-sensitive fluorescent dye, JC-1 (Thermo Fisher Scientific), following the manufacturer's instructions. Cells were collected and suspended in PBS at 1×10^6 cells/ml containing JC-1 and incubated at 37 °C, 5% CO_2 for 30 min. Cells were washed twice with PBS and analyzed by flow cytometry (FACS Caliber, Becton Dickinson). The JC-1 monomer (green) and the J-aggregates (red) were detected separately in FL1 (emission, 525 nm) and FL2 (emission, 590 nm) channels, respectively. The red to green emission ratio provided an estimate of ΔΨm.

Cell fractionation

Mitochondrial and cytosolic fractions were prepared using the Cell Fractionation Kit according to the manufacturer's instructions (Abcam, MA). Equal amounts of proteins were subjected to electrophoresis and immunoblot analysis.

Comet assay

Cells were washed with PBS and embedded in a 1% low-melting agarose on slides, lysed, and electrophoresed under neutral conditions (Supplementary Materials and Methods). Slides were placed in a DNA precipitation solution, dried, and stained with ethidium bromide and imaged on phase contrast microscope (Olympus, Tokyo, Japan). At least 50 cells were analyzed per condition using the OpenComet software [37].

Seahorse extracellular flux analysis

OCR and ECAR of live cells were measured using a Seahorse Bioscience XF96 Extracellular Flux Analyzer (Supplementary Materials and Methods). Seahorse programming consisted of four 3-min baseline measurements with 1-min intervals, which were repeated after each injection. All values were normalized to DNA content of each well to account for growth differences.

ROS detection assay

Cellular ROS detection assay (Abcam PLC, Cambridge, MA, USA) and MitoSOX™ mitochondrial ROS indicator (Thermo Fisher Scientific) were used to measure total and mitochondrial ROS activity following the manufacturer's instructions. After cells were incubated 2′,7′-dichlorofluorescein diacetate and MitoSOX red regent at 37 °C for 1 h, cells were analyzed on FACS Calibur flow cytometer (BD Biosciences). Relative fluorescence intensities were analyzed, and histograms were generated using FlowJo 10.4.1 software.

Metabolomics

An unbiased, metabolomic profiling analysis was conducted using UPLC-MS mass spectrometry (Metabolon Inc., NC) (Supplementary Materials and Methods). Metabolites were mapped to pathways based on MetaboAnalyst, a comprehensive online tool suited for

metabolomic data analysis (www.metaboanalyst.ca) [38]. A summary of the biochemical products that achieved statistical significance is reported ($p \leq 0.05$).

Transcriptome analysis

RNA was used to create libraries according to the protocol (Supplementary Materials and Methods). Differential gene expression analyses (DEGs) were investigated and mapped for canonical pathways by IPA (Ingenuity Systems, USA). For GSEA, the preranked gene list was created based on the values derived from dividing the log *p*-values by the log fold changes as determined in the DEGs.

BH3 profiling

BH3 profiling was tested following the published protocol by the Letai laboratories [39]. Peptides of about 20 amino acids that correspond to the active (BH3) domain of multiple antiapoptotic activators and sensitizers (BIM, PUMA, BAD, NoxaA, MS1, HRK) were incubated at multiple concentrations with harvested cells for 1 h at room temperature. Anti-cytoC staining was performed at 4 °C overnight and FACS analysis was performed 16 h after peptide exposure. Retained cytoC is measured and percent release is calculated (Supplementary Materials and Methods).

Statistical analysis

Quantitative data were presented as the mean ± SD. The Student *t* test compared means between the two groups. One-way ANOVA followed by the post hoc Dunnett test compared means of more than two group, and a multiple range least significant difference was used for intergroup comparisons. Survival curves were plotted by the Kaplan-Meier method, and compared by the log-rank test (*,$^{\Delta}P < 0.05$; **,$^{\Delta\Delta}P < 0.01$). All statistical analyses were performed with SPSS 16.0 and Graph Pad.

Supplementary Material

Refer to Web version on PubMed Central for supplementary material.

Acknowledgements

The authors thank Dr Chuan-Yuan Li, Duke University, for the kind gift of the caspase 3 reporter plasmid and Dr Jeremy Ryan and Dr Anthony Letai for BH3 profiling support.

References

1. Siegel RL, Miller KD, Jemal A. Cancer statistics, 2018. CA Cancer J Clin. 2018;68:7–30. [PubMed: 29313949]
2. Hur C, Miller M, Kong CY, Dowling EC, Nattinger KJ, Dunn M, et al.Trends in esophageal adenocarcinoma incidence and mortality. Cancer. 2013;119:1149–58. [PubMed: 23303625]
3. Kong CY, Kroep S, Curtius K, Hazelton WD, Jeon J, Meza R, et al.Exploring the recent trend in esophageal adenocarcinoma incidence and mortality using comparative simulation modeling. Cancer Epidemiol Biomark Prev. 2014;23:997–1006.
4. Sobieraj DM, Coleman SM, Coleman CI. US prevalence of upper gastrointestinal symptoms: a systematic literature review. Am J Manag Care. 2011;17:e449–158. [PubMed: 22200062]

5. Runge TM, Abrams JA, Shaheen NJ. Epidemiology of Barrett's esophagus and esophageal adenocarcinoma. Gastroenterol Clin North Am. 2015;44:203–31. [PubMed: 26021191]
6. Yen CJ, Izzo JG, Lee DF, Guha S, Wei Y, Wu TT, et al.Bile acid exposure up-regulates tuberous sclerosis complex 1/mammalian target of rapamycin pathway in Barrett's-associated esophageal adenocarcinoma. Cancer Res. 2008;68:2632–10. [PubMed: 18413730]
7. Ichim G, Lopez J, Ahmed SU, Muthalagu N, Giampazolias E, Delgado ME, et al.Limited mitochondrial permeabilization causes DNA damage and genomic instability in the absence of cell death. Mol Cell. 2015;57:860–72. [PubMed: 25702873]
8. Liu X, He Y, Li F, Huang Q, Kato TA, Hall RP, et al.Caspase-3 promotes genetic instability and carcinogenesis. Mol Cell. 2015;58:284–96. [PubMed: 25866249]
9. Westphal D, Dewson G, Czabotar PE, Kluck RM. Molecular biology of Bax and Bak activation and action. Biochim Biophys Acta. 2011;1813:521–31. [PubMed: 21195116]
10. Tait SW, Green DR. Mitochondria and cell death: outer membrane permeabilization and beyond. Nat Rev Mol Cell Biol. 2010;11:621–32. [PubMed: 20683470]
11. Gillies LA, Kuwana T. Apoptosis regulation at the mitochondrial outer membrane. J Cell Biochem. 2014;115:632–40. [PubMed: 24453042]
12. Hanahan D, Weinberg RA. Hallmarks of cancer: the next generation. Cell. 2011;144:646–74. [PubMed: 21376230]
13. Yi X, Yin XM, Dong Z. Inhibition of Bid-induced apoptosis by Bcl-2. tBid insertion, Bax translocation, and Bax/Bak oligomerization suppressed. J Biol Chem. 2003;278:16992–9. [PubMed: 12624108]
14. Spencer SL, Sorger PK. Measuring and modeling apoptosis in single cells. Cell. 2011;144:926–39. [PubMed: 21414484]
15. Xu Y, Feingold PL, Surman DR, Brown K, Xi S, Davis JL, et al.Bile acid and cigarette smoke enhance the aggressive phenotype of esophageal adenocarcinoma cells by downregulation of the mitochondrial uncoupling protein-2. Oncotarget. 2017;8:101057–71. [PubMed: 29254145]
16. Bajpai M, Aviv H, Das KM. Prolonged exposure to acid and bile induces chromosome abnormalities that precede malignant transformation of benign Barrett's epithelium. Mol Cytogenet. 2012;5:43. [PubMed: 23194200]
17. Tang HL, Tang HM, Mak KH, Hu S, Wang SS, Wong KM, et al.Cell survival, DNA damage, and oncogenic transformation after a transient and reversible apoptotic response. Mol Biol Cell. 2012;23:2240–52. [PubMed: 22535522]
18. Lovric MM, Hawkins CJ. TRAIL treatment provokes mutations in surviving cells. Oncogene. 2010;29:5048–60. [PubMed: 20639907]
19. Potter DS, Letai A. To prime, or not to prime: that is the question. Cold Spring Harb Symp Quant Biol. 2016;81:131–10. [PubMed: 27811212]
20. Beroukhim R, Mermel CH, Porter D, Wei G, Raychaudhuri S, Donovan J, et al.The landscape of somatic copy-number alteration across human cancers. Nature. 2010;463:899–905. [PubMed: 20164920]
21. Williams MM, Lee L, Hicks DJ, Joly MM, Elion D, Rahman B, et al.Key survival factor, Mcl-1, correlates with sensitivity to combined Bcl-2/Bcl-xL blockade. Mol Cancer Res. 2017;15:259–68. [PubMed: 28039357]
22. Ertel F, Nguyen M, Roulston A, Shore GC. Programming cancer cells for high expression levels of Mcl1. EMBO Rep. 2013;14:328–36. [PubMed: 23478333]
23. Perciavalle RM, Opferman JT. Delving deeper: MCL-1's contributions to normal and cancer biology. Trends Cell Biol. 2013;23:22–29. [PubMed: 23026029]
24. Rezaei Araghi R, Bird GH, Ryan JA, Jenson JM, Godes M, Pritz JR, et al.Iterative optimization yields Mcl-1-targeting stapled peptides with selective cytotoxicity to Mcl-1-dependent cancer cells. Proc Natl Acad Sci USA. 2018;115:E886–E895. [PubMed: 29339518]
25. Tait SW, Green DR. Mitochondrial regulation of cell death. Cold Spring Harb Perspect Biol. 2013;5:a008706. [PubMed: 24003207]
26. Kwong JQ, Henning MS, Starkov AA, Manfredi G. The mitochondrial respiratory chain is a modulator of apoptosis. J Cell Biol. 2007;179:1163–77. [PubMed: 18086914]

27. Sabharwal SS, Schumacker PT. Mitochondrial ROS in cancer: initiators, amplifiers or an Achilles' heel?Nat Rev Cancer. 2014;14:709–21. [PubMed: 25342630]

28. Weinberg F, Hamanaka R, Wheaton WW, Weinberg S, Joseph J, Lopez M, et al.Mitochondrial metabolism and ROS generation are essential for Kras-mediated tumorigenicity. Proc Natl Acad Sci USA. 2010;107:8788–93. [PubMed: 20421486]

29. Yadav N, Kumar S, Marlowe T, Chaudhary AK, Kumar R, Wang J, et al.Oxidative phosphorylation-dependent regulation of cancer cell apoptosis in response to anticancer agents. Cell Death Dis. 2015;6:e1969. [PubMed: 26539916]

30. Byun JY, Kim MJ, Eum DY, Yoon CH, Seo WD, Park KH, et al.Reactive oxygen species-dependent activation of Bax and Poly (ADP-ribose) polymerase-1 is required for mitochondrial cell death induced by triterpenoid pristimerin in human cervical cancer cells. Mol Pharm. 2009;76:734–44.

31. Kim MJ, Yun HS, Hong EH, Lee SJ, Baek JH, Lee CW, et al.Depletion of end-binding protein 1 (EB1) promotes apoptosis of human non-small-cell lung cancer cells via reactive oxygen species and Bax-mediated mitochondrial dysfunction. Cancer Lett. 2013;339:15–24. [PubMed: 23900080]

32. Li DC, Ueta E, Kimura T, Yamamoto T, Osaki T. Reactive oxygen species (ROS) control the expression of Bcl-2 family proteins by regulating their phosphorylation and ubiquitination. Cancer Sci. 2004;95:644–50. [PubMed: 15298726]

33. Hormi-Carver K, Zhang X, Zhang HY, Whitehead RH, Terada LS, Spechler SJ, et al.Unlike esophageal squamous cells, Barrett's epithelial cells resist apoptosis by activating the nuclear factor-kappa B pathway. Cancer Res. 2009;69:672–7. [PubMed: 19147583]

34. Huo X, Juergens S, Zhang X, Rezaei D, Yu C, Strauch ED, et al.Deoxycholic acid causes DNA damage while inducing apoptotic resistance through NF-kappaB activation in benign Barrett's epithelial cells. Am J Physiol Gastrointest Liver Physiol. 2011;301:G278–286. [PubMed: 21636532]

35. Kotschy A, Szlavik Z, Murray J, Davidson J, Maragno AL, Le Toumelin-Braizat G, et al.The MCL1 inhibitor S63845 is tolerable and effective in diverse cancer models. Nature. 2016;538:477–82. [PubMed: 27760111]

36. Palanca-Wessels MC, Barrett MT, Galipeau PC, Rohrer KL, Reid BJ, Rabinovitch PS. Genetic analysis of long-term Barrett's esophagus epithelial cultures exhibiting cytogenetic and ploidy abnormalities. Gastroenterology. 1998;114:295–304. [PubMed: 9453489]

37. Gyori BM, Venkatachalam G, Thiagarajan PS, Hsu D, Clement MV. OpenComet: an automated tool for comet assay image analysis. Redox Biol. 2014;2:457–65. [PubMed: 24624335]

38. Chong J, Soufan O, Li C, Caraus I, Li S, Bourque G, et al.MetaboAnalyst 4.0: towards more transparent and integrative metabolomics analysis. Nucleic Acids Res. 2018;46:W486–W494. [PubMed: 29762782]

39. Ryan J, Montero J, Rocco J, Letai A. iBH3: simple, fixable BH3 profiling to determine apoptotic priming in primary tissue by flow cytometry. Biol Chem. 2016;397:671–8. [PubMed: 26910743]

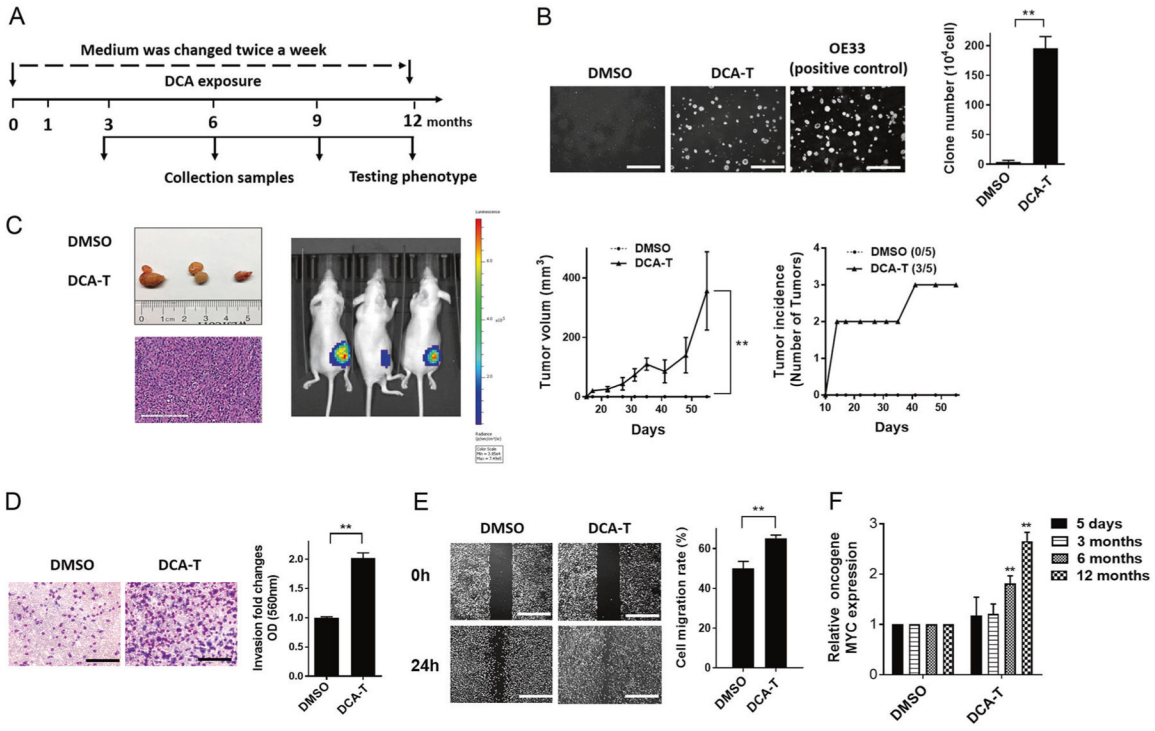

Fig. 1.

The bile acid, DCA, induces carcinogenesis in dysplastic Barrett's epithelial cells. **a** Cells were cultured for 12 months with twice weekly changes in media containing DCA or DMSO. Cells were harvested at 3, 6, 9, and 12 months. **b** The colonies in soft agar were photographed and counted (mean ± SD) as three independent experiments (scale bar = 250 μm). **c** 12-month exposed cells were injected subcutaneously into flanks of nude mice (five mice/ten flanks per experiment) with stable luciferase reporter transfection. Left flank is DMSO and right is DCA group. H&E staining of biopsy specimens from DCA group and images of tumor-bearing mice. Three independent experiments were performed with similar results. **d** Invasion was determined by transwell assays with representative images shown (scale bar = 50 μm). Quantitative analysis of invasion was measured by absorbance at OD 560 nm after staining with crystal violet. Fold changes (mean ± SD) were obtained from three independent experiments. **e** The cell migration was analyzed by wound-healing assays. Photographs were obtained at 0 and 24 h (scale bar = 125 μm). Covered areas by migrated cells in the nine random fields after exposure were quantified by Image J software. **e** qRT-PCR analysis of oncogene MYC expression normalized with actin (*$P < 0.05$ and **$P < 0.01$)

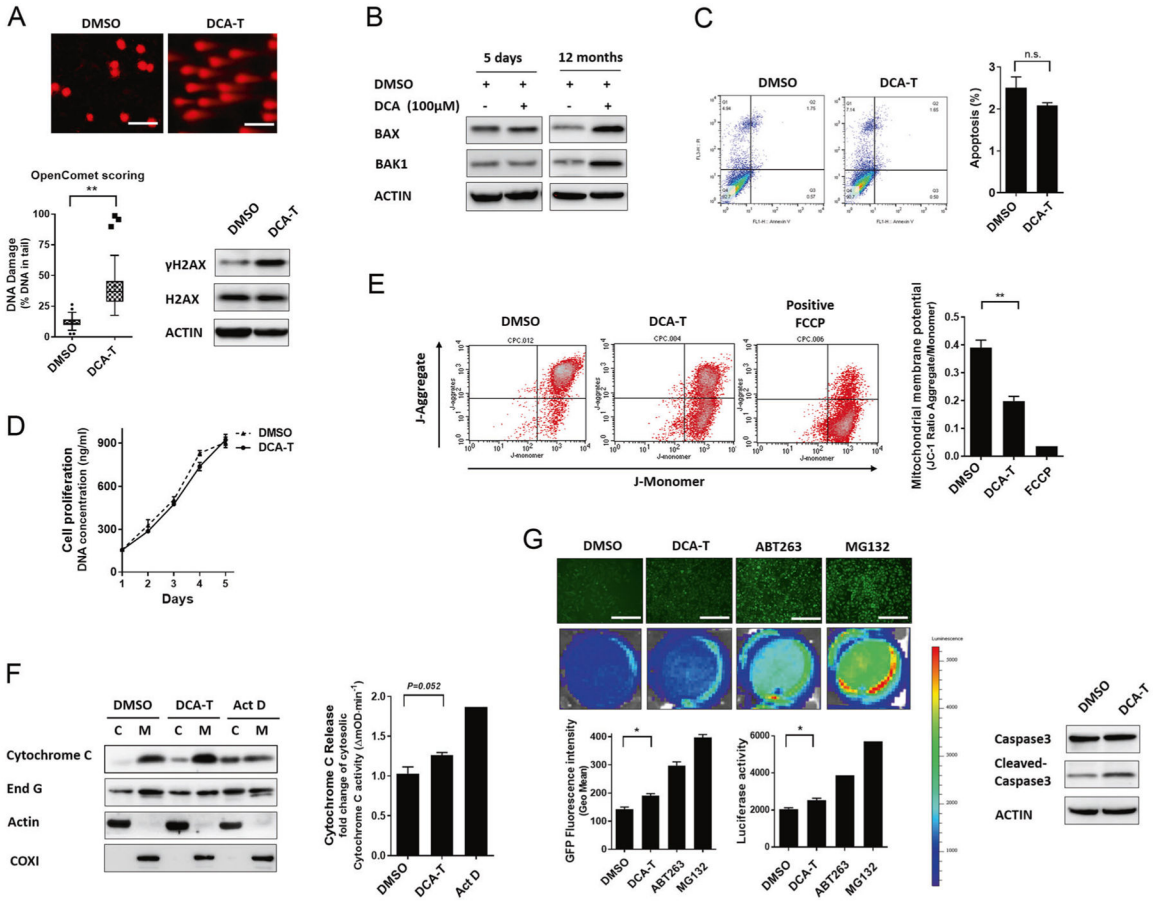

Fig. 2.

DCA induces “Minority MOMP” in transformed BE cells. **a** DNA damage was examined by the comet assay using fluorescence microscopy (scale bar = 25 μm). The percentage of DNA in the tail is plotted as determined by OpenComet (*$P < 0.05$ and **$P < 0.01$). The protein levels of γH2AX were analyzed by immunoblots. **b** Protein levels of Bax and Bak1 were analyzed by immunoblots after 5 days and 12 months. **c** Cells were stained with annexin V and PI and analyzed by FACS. Cells positive for annexin V staining were counted as apoptotic cells. **d** Cell proliferation was measured by the CyQuant assay, in which DNA concentration is measured as a surrogate for cell numbers. **e** Analysis of mitochondrial membrane potentials (ΔΨm) using flow cytometry with JC-1 dye. Loss of ΔΨm was demonstrated by the change in JC-1 fluorescence from red (JC-1 aggregates) to green (JC-1 monomers) represented as ratio of JC-1 red to green fluorescence. **f** Immunoblots for cytoC were performed on the mitochondrial and cytosolic fractions. The ELISA assay showing activities of cytoC in cytosolic fractions with actinomycin D (ActD) as positive control. **g** Cells with caspase 3 reporter were treated with positive controls, ABT-263 (10 μM, induces apoptosis), or MG132 (10 μM, inhibits proteasome). Luciferase activities and EGFP shown in representative images (scale bar = 125 μm)

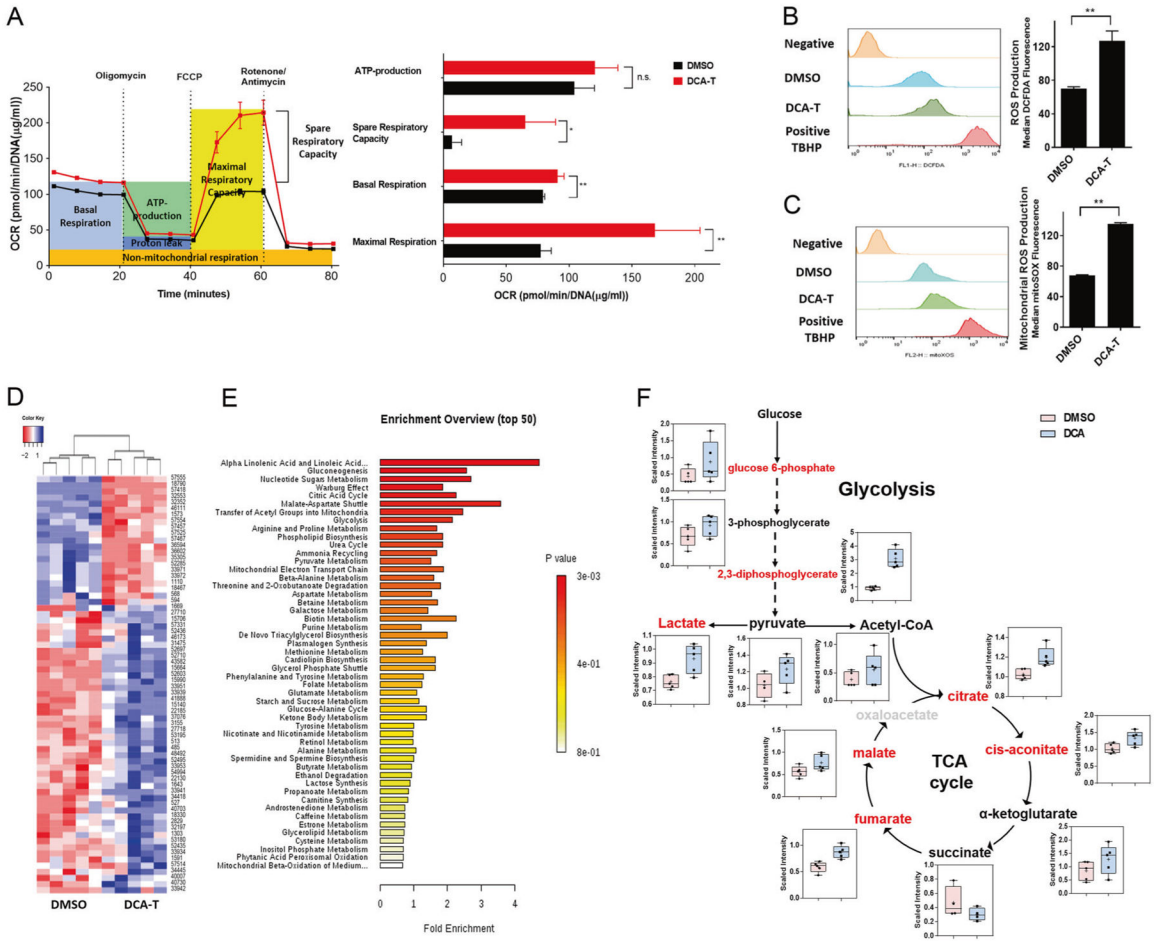

Fig. 3.

Altered mitochondrial function and global metabolomic signatures in DCA transformed BE cells. **a** Oxygen consumption rate (OCR) was measured with sequential injections of oligomycin, FCCP, and rotenone/antimycin at the time points indicated. Basal Respiratory capacity, maximal respiration, and ATP production were calculated as described in Supplementary Materials and Methods section. **b** The level of cellular ROS was measured using DCFDA fluorescence by flow cytometry with the median of fluorescence ± SD analyzed using FlowJo software (** $P < 0.01$). **c** Mitochondrial ROS concentrations was measured using MitoSOX™ Red reagent by flow cytometry with the median of fluorescence ± SD analyzed using FlowJo software (** $P < 0.01$). **d** Heatmap representation of 68 metabolites (List in Supplementary Table 1) between the DCA and DMSO groups in clustering analysis. Each line represents a metabolite. **e** Metabolic pathway analyses of differentially secreted metabolites in DCA and DMSO groups utilizing the MetaboAnalyst functional interpretation tools. The horizontal bars summarize the main metabolite sets identified; bars are colored based on *p*-values and length is based on fold enrichment. **f** Box plots illustrating the observed metabolites involved in glycolysis, and TCA cycle in DCA-T (blue bars) compare with DMSO (pink bars). Metabolites in red exhibit concentrations significantly increased in DCA-T compared with DMSO

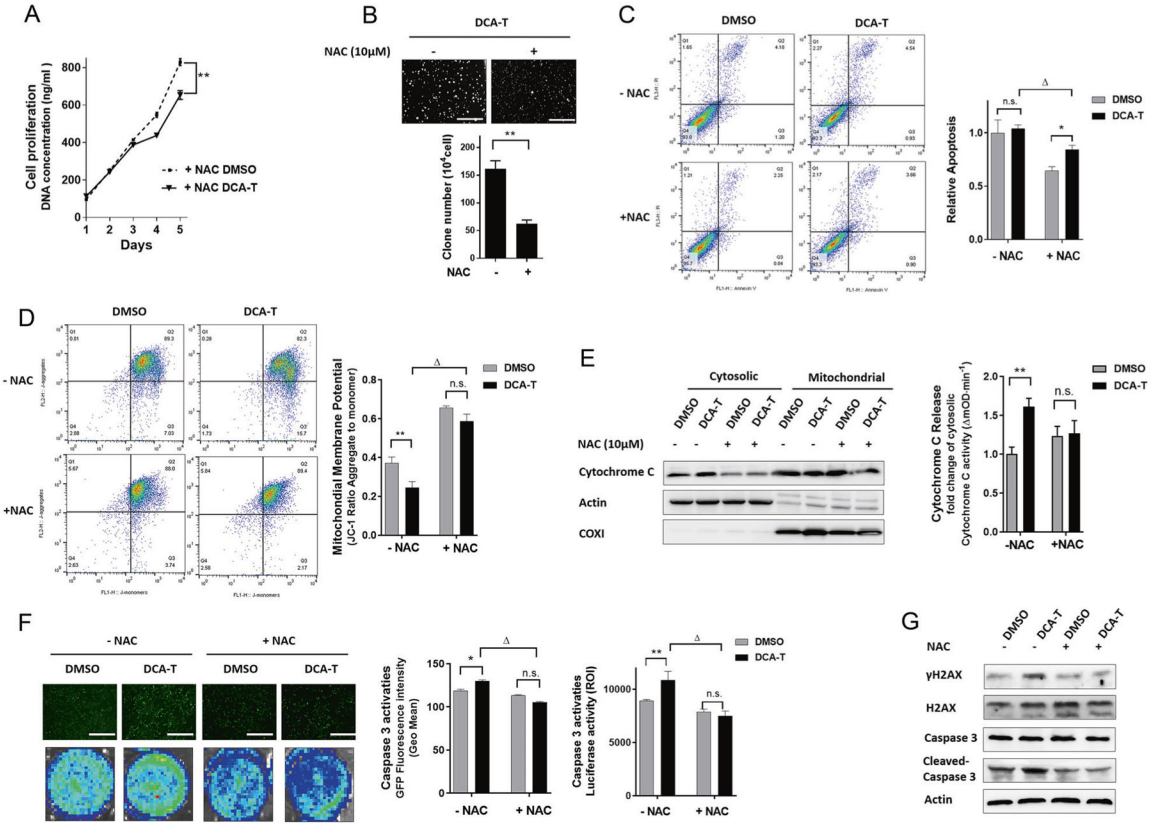

Fig. 4.

ROS production is linked with "Minority MOMP." **a** Cell proliferation was measured by the CyQuant assay (**$P < 0.01$). **b** The colonies in soft agar were photographed and counted (mean ± SD) in DCA-T cells with or without NAC (**$P < 0.01$). **c** Cells were stained with annexin V and PI and analyzed by FACS. Cells positive for annexin V staining were counted as apoptotic cells (*$P < 0.05$ for DMSO versus NAC; $^{\Delta}P < 0.05$ for DCA-T without NAC). **d** Analysis of ΔΨm using flow cytometry with JC-1 dye. Loss of ΔΨm was shown as a ratio (**$P < 0.01$ as compare with DMSO, $^{\Delta}P < 0.05$ as compare with DCA-T without NAC treatment). **e** After NAC treatment, immunoblots for cytoC were performed on mitochondrial and cytosolic fractions. The ELISA assay showing activities of cytoC in cytosolic fractions. **f** Cells with caspase 3 reporter were treated with NAC, ABT-737 (10 μM), or MG132 (10 μM). The growth of cells as observed by the EGFP activity. Representative images from florescence imaging, original magnification ×40, scale bar = 125 μm. (*$P < 0.05$, **$P < 0.01$ as compare with DMSO groups, $^{\Delta}P < 0.05$ as compare with DCA-T without NAC treatment). **g** The protein levels of γH2AX, Caspase 3, and cleaved-caspase 3 were analyzed by immunoblots

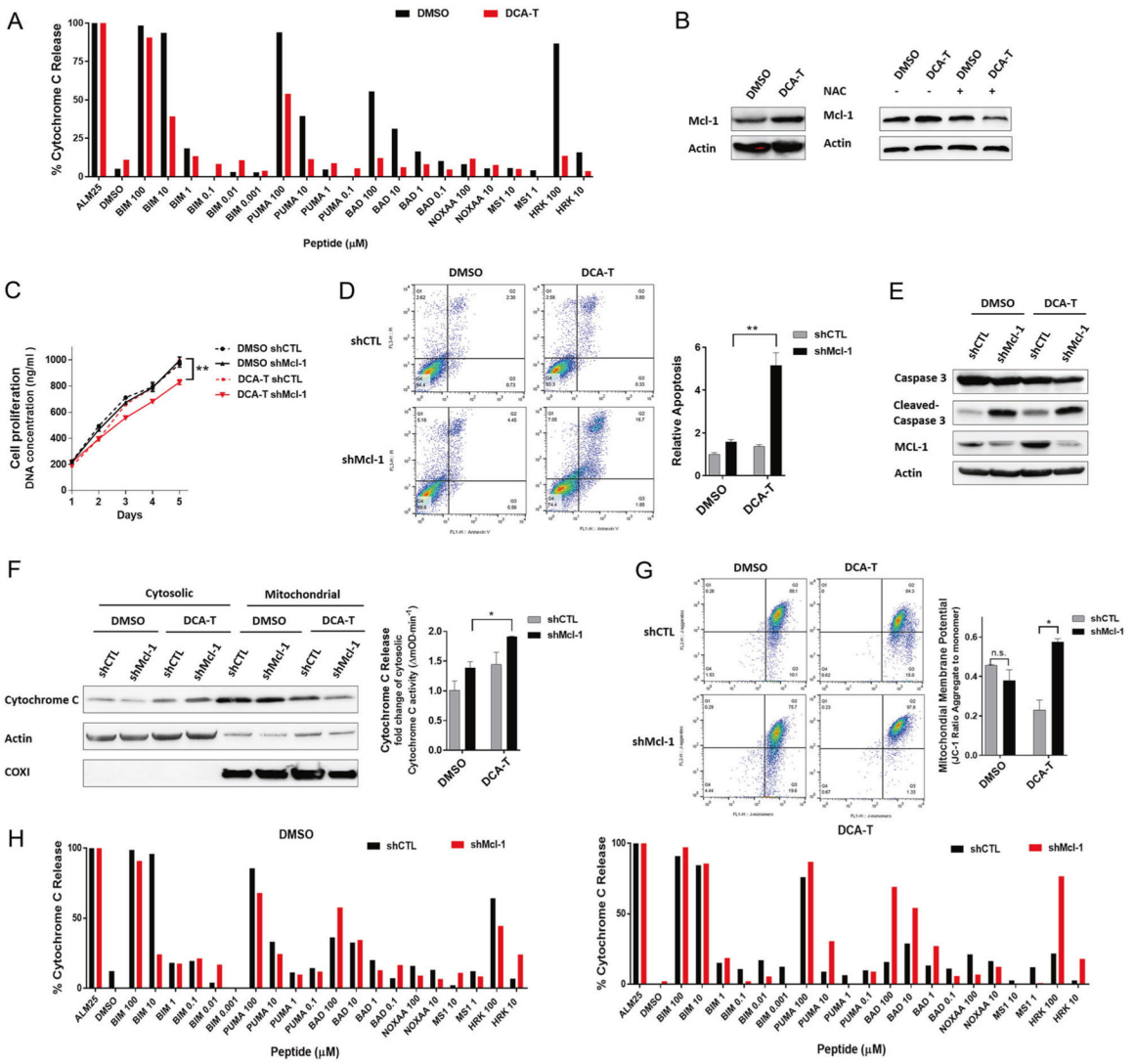

Fig. 5.

Mcl-1 provides a resistance balance to DCA induced-minority MOMP. **a** Comparison of BH3 profiling in DMSO and DCA-T cells. **b** Mcl-1 expression was analyzed by immunoblots after 10 μM NAC pretreated of DCA-T and DMSO group cells for 6 h. Stable knockdown of Mcl-1 (shMcl-1) or scrambled control (shCTL) was generated by transfecting short-hairpin RNA lentiviruses. **c** Cell proliferation was measured by the CyQuant assay (**$P < 0.01$). **d** Cells were stained with annexin V and PI and analyzed by FACS. Cells positive for annexin V staining were counted as apoptotic cells (**$P < 0.01$). **e** The protein levels of Mcl-1, Caspase 3, and cleaved-caspase 3 were analyzed by immunoblots. **f** Immunoblots for cytoC were performed on the mitochondrial and cytosolic fractions. The ELISA assay showing activities of cytoC in cytosolic fractions (**$\mathbf{P} < 0.01$). **g** Analysis of ΔΨm were performed using flow cytometry with JC-1 dye. The data (mean ± SD) showed the ratio of JC-1 red fluorescence to green fluorescence (*$P < 0.05$). **h** BH3 profiles in different cell conditions

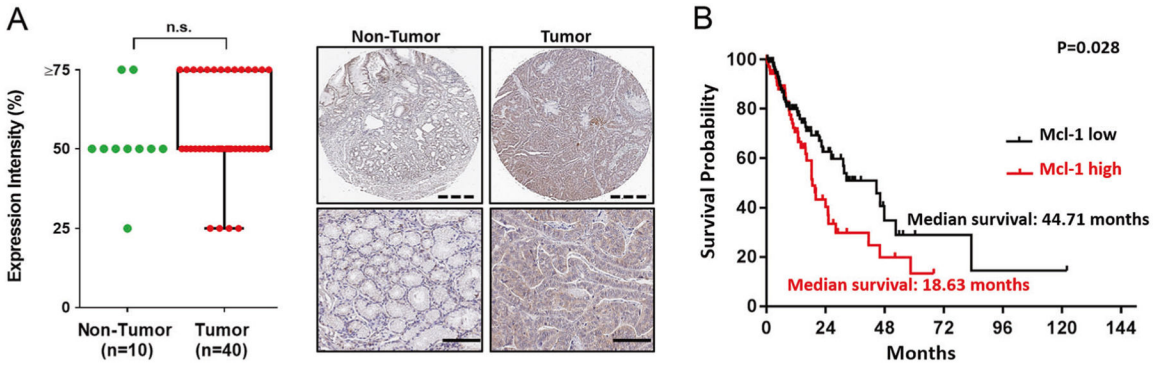

Fig. 6.

Mcl-1 expression is upregulated in esophageal cancer tissue and is associated with poor patient prognosis. **a** Samples were categorized into four levels of expression patterns. ten normal esophageal tissues were compared with forty tumor samples from a US Biomax microarray. The brown staining indicates Mcl-1 expression in a representative sample (scale bar = 100 μm). **b** Kaplan–Meier survival curve for overall survival of patients with low and high expression of Mcl-1 based on mRNA from The Cancer Genome Atlas (TCGA) dataset

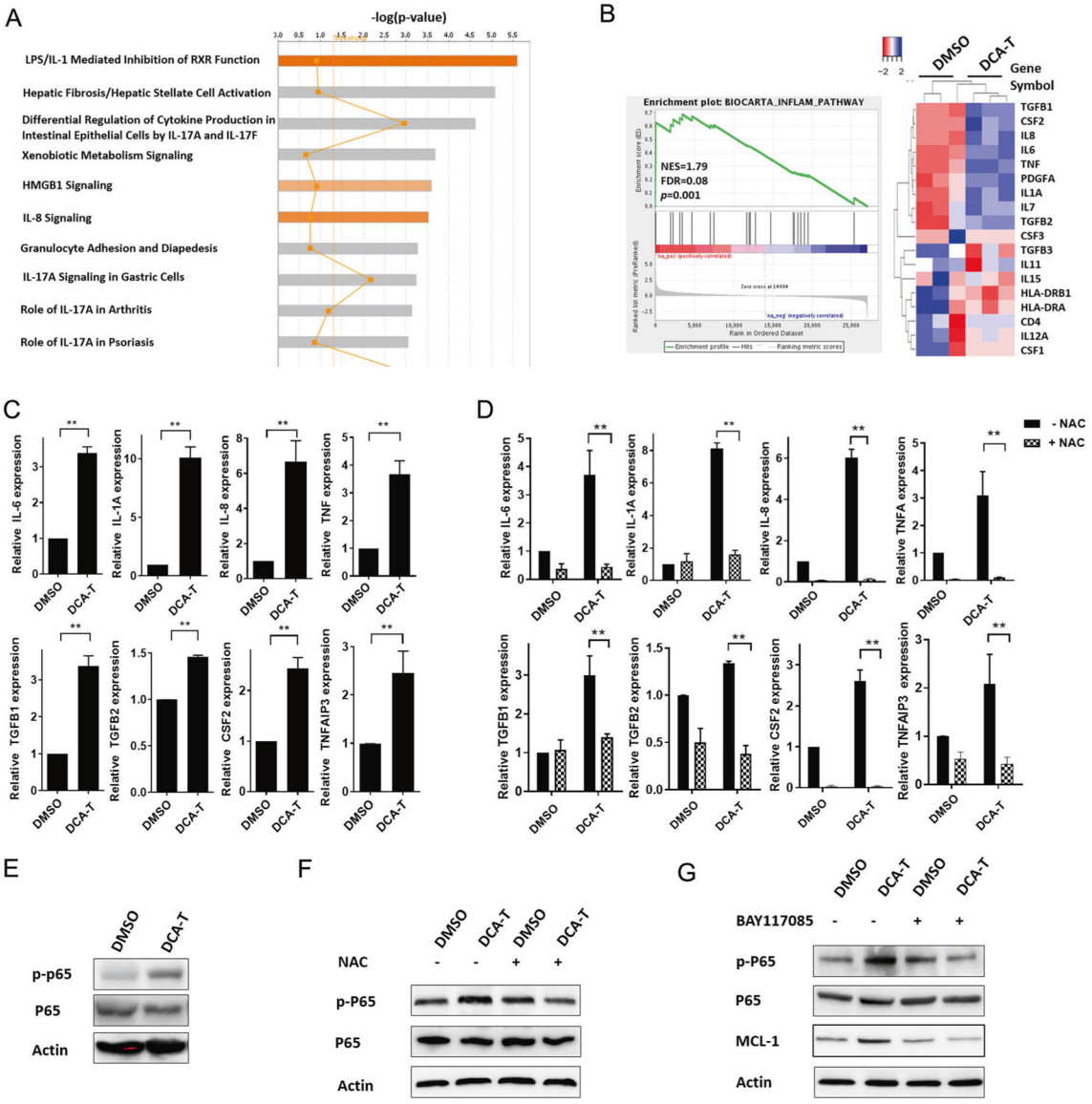

Fig. 7.

Inflammation and NF-κB activation contribute to Mcl-1 upregulation. **a** Ingenuity Pathway Analysis (IPA) was performed from RNA-seq data and arranged by signaling pathways in order of statistical significance with top ten pathways shown (gene expression in Supplementary Table 2). **b** Enrichment plot and heatmap for the gene set of inflammatory genes between DMSO and DCA-T group. The green curve represents the evolution of the density of the genes identified in the RNA-seq. Heatmap showing enriched genes in inflammation and RELA GSEA. NES normalized enrichment score, p nominal *p*-value, FDR false discovery rate. **c** qRT-PCR analysis was used to validate gene expression changes in the "inflammation pathway" identified by GSEA (***P* < 0.01). **d** qRT-PCR analysis of inflammation related genes expression normalized with actin after 6 h of 10 μM NAC pretreatment (***P* < 0.01 as compare with DCA-T group without NAC treatment). **e** Immunoblot of phosphorylated-p65 (p-p65) and p65. **f** Immunoblot of phosphorylated-

p65 (p-p65) and p65 after 6 h of 10 μM NAC pretreatment. **g** Immunoblots of MCL-1, phosphorylated-p65 (p-p65), and p65 after 10 μM of BAY117085 (inhibitor of NF-κB) pretreatment

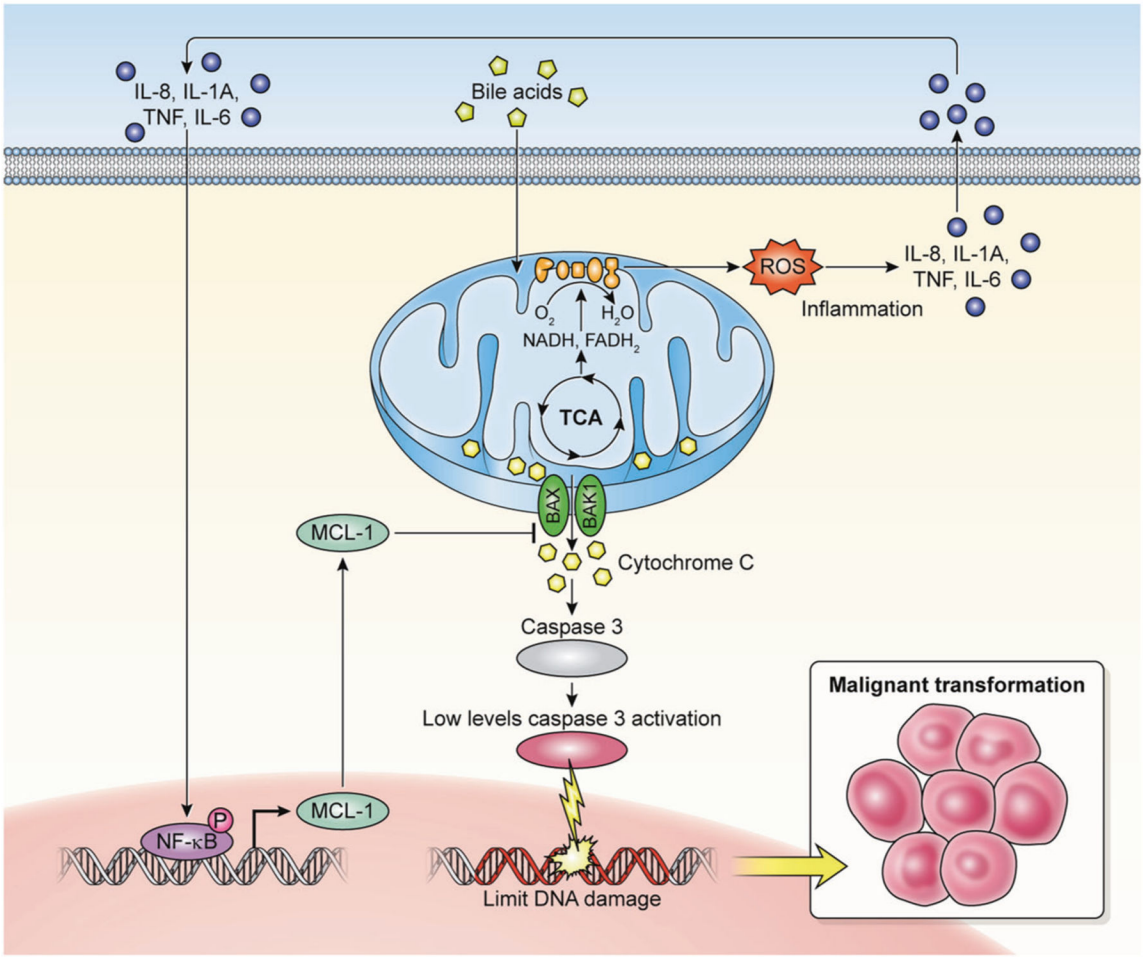

Fig. 8.

Proposed mechanism of minority MOMP induced by DCA. Upregulation of Mcl-1 due to DCA exposure activates the NF-κB signaling pathway through inflammatory reaction that provides a balance to the mitochondrial preventing widespread MOMP. Minority MOMP cause limited cytoC release, low levels of caspases-3 activation, and limited DNA damage which are insufficient to trigger cell death but sufficient promote oncogenic transformation and tumorigenesis